Geologica Acta, Vol.13, Nº4, December 2015, 263-278
DOI: 10.1344/GeologicaActa2015.13.4.1

geologica acta

Geochemistry of Precordillera serpentinites, western Argentina: evidence for multistage hydrothermal alteration and tectonic implications for the Neoproterozoic–early Paleozoic

F.L. BOEDO[1] M.P. ESCAYOLA[1] S.B. PÉREZ LUJÁN[2] G.I. VUJOVICH[1] J.P. ARIZA[3] M. NAIPAUER[1]

[1]Instituto de Estudios Andinos "Don Pablo Groeber" (UBA-CONICET). Departamento de Ciencias Geológicas, Facultad de Ciencias Exactas y Naturales, Universidad de Buenos Aires
Boedo E-mail: florenciaboedo@gmail.com Escayola E-mail: mescayola@gl.fcen.uba.ar
Vujovich E-mail: graciela@gl.fcen.uba.ar Naipauer E-mail: maxinaipauer@gl.fcen.uba.ar

[2]CONICET-Departamento de Geofísica y Astronomía, Facultad de Ciencias Exactas, Físicas y Naturales, Universidad Nacional de San Juan, Argentina
E-mail: sofiap.lujan@unsj-cuim.edu.ar

[3]Instituto Geofísico Sismológico Volponi (UNSJ-CONICET). Universidad Nacional de San Juan, Argentina
E-mail: jpariza@conicet.gov.ar

ABSTRACT

Serpentinites are a powerful tool to evaluate mantle composition and subsequent alteration processes during their tectonic emplacement. Exposures of this type of rocks can be found in the Argentine Precordillera (Cuyania terrane) and Frontal Cordillera, both located in central-western Argentina, within the Central Andes. In these regions a Neoproterozoic to Devonian mafic-ultramafic belt composed of serpentinites, metabasaltic dikes/sills, pillow lavas (with an Enriched to Normal Mid-Ocean Ridge Basalts (E- to N-MORB) geochemical signature) and mafic granulites crop out, spatially associated with marine metasedimentary rocks. The serpentinite bodies consist of lizardite/chrysotile+brucite+magnetite, with scarce pentlandite and anhedral reddish-brown Cr-spinel (picotite, pleonaste and spinel sensu stricto) as relict magmatic phases. The original peridotites were moderately-depleted harzburgites (ultramafic cumulates) with an intermediate chemical signature between a mid-ocean ridge and an arc-related ophiolite. Whole-rock Rare Earth Elements (REE) patterns of serpentinites exhibit enriched REE patterns ((La/Yb)CN=13-59) regarding CI chondrite with positive Eu anomalies. These features are the result of an interaction between hydrothermal fluid and serpentinites, in which moderate temperature (350º–400ºC), CO_2-rich, mildly basic hydrothermal fluid was involved and was responsible for the addition of Ca, Sr and REE to serpentinites. The presence of listvenites (silica-carbonate rocks) in the serpentinite margins allow us to infer another fluid metasomatism, where low-temperatures (<250ºC), highly-oxidized, highly-acid fluid lead to the precipitation of silica. The association of these metasomatized serpentinite bodies with neoproterozoic continental margin sucessions and MORB magmatism at the suture zone of the Cuyania and Chilenia terranes suggests the development of an oceanic basin between them during the Neoproterozoic-early Paleozoic.

KEYWORDS **Mafic-ultramafic belt. Mid-ocean ridge. Listvenites. Cuyania terrane. Chilenia terrane.**

INTRODUCTION

Mantle rocks tectonically emplaced in orogenic belts provide information about the composition of the mantle and processes that occurred during its formation. Due to the large scale of these processes, they provide information by ultramafic xenoliths, allowing, for example, observation of the relationships between lithologies, evaluation of the mantle heterogeneity scale and analysis of magmatic/metamorphic processes (vein injections, melt-rock reactions, etc.). However, when rock bodies are affected by deformation and metamorphism, their original geodynamic setting is not exactly known and their significance is sometimes a subject of speculation (Bodinier and Godard, 2003). In this case, only relic primary mantle minerals, in particular Cr-spinel, constitute a good petrogenetic indicator that gives information about origin and petrogenesis of mantle peridotite before serpentinization (Pearce *et al*., 2000; Arai *et al*., 2011, among others).

Deformational, metamorphic and metasomatic processes can become a fundamental tool for the study of secondary processes. Metasomatic products (metasomatites) are related to the nature of host rocks and the composition of the circulating fluid and are important subjects of mineral research and exploration, since they are valuable indicators for exploration geologists. In particular, the interaction of hydrothermal fluids with ultramafic rocks results in a variety of metasomatic rocks such as quartz-carbonate rocks and serpentine-talc-carbonate rocks. The term "listvenite" was introduced by Rose (1837) to describe silica-carbonate-chromium mica rocks associated with gold-bearing quartz veins. Listvenites are chiefly composed of carbonate (magnesite, dolomite, ankerite), quartz and Cr-mica (mariposite, fuchsite) with disseminated pyrite (Halls and Zhao, 1995) and minor chlorite, and talc. Relic serpentines and Cr-spinel are also found. They are generated by the interaction between intermediate to low temperature hydrothermal/metasomatic alteration of mafic-ultramafic rocks and can be associated with structures (faults, shear zones) or to granitic plutons (Halls and Zhao, 1995; Robinson *et al*., 2005).

This contribution deals with the alteration products and with relics of primary minerals such as Cr-spinels in an effort to understand the history of the Argentine Precordillera serpentinite bodies, from their tectonic setting of formation to the conditions of metamorphic and metasomatic (listvenitization) processes.

GEOLOGY OF THE ARGENTINE PRECORDILLERA

Geological outline

The southwestern margin of the South American plate (28º–33ºSL, Fig. 1A) is a natural laboratory where the tectonic evolution of Gondwana can be observed and analyzed. During early Paleozoic times, the western margin of the continent grew by the accretion of different terranes (Pampia, Cuyania, Chilenia) (Ramos, 2010 and others mentioned therein). Several authors have concluded that the Cuyania terrane (Argentine Precordillera) represents a microcontinent that broke up from southern Laurentia in the early Cambrian and collided against the Gondwana margin during the Late Ordovician (Dickerson, 2012; Thomas *et al*., 2012). However, the evolution of the western margin of the Cuyania terrane during early Paleozoic times is still a matter of debate. There is a general consensus that during this time span a passive margin setting was developed in association with a shallow ocean basin to the west, which was closed during Middle–Late Devonian times by the collision of the Chilenia terrane against the Gondwana margin (the Cuyania terrane). Different proposed tectonic models (Ramos *et al*., 1986; Dalla Salda *et al*., 1992; Loeske, 1993; Davis *et al*., 1999, 2000, among others) highlight the remaining uncertainties because of the few studies focusing on issues such as the early Paleozoic deformation (Cucchi, 1972; Von Gosen, 1997; Davis *et al*.,

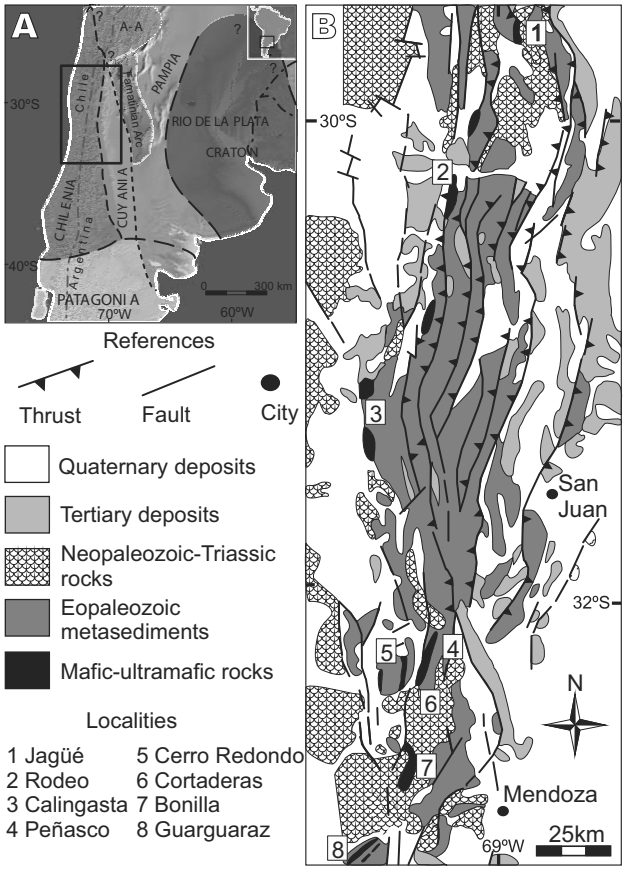

FIGURE 1. A) Location of the Chilenia and Cuyania terranes. A-A: Arequipa-Antofalla terrane. Diagram taken from Abre *et al.* (2012). B) Schematic geological map and localities of the Argentine Precordillera mafic-ultramafic belt (after Ramos *et al.*, 2000).

1999; Gerbi *et al.*, 2002), the polarity of the subduction zone between the Chilenia terrane and the Gondwana margin, or the origin and emplacement of the Argentine Precordillera mafic-ultramafic belt, considered as the suture zone between the Chilenia and Cuyania terranes (Haller and Ramos, 1984; Kay *et al.*, 1984; Davis *et al.*, 1999, 2000, among others).

Geology of the Argentine Precordillera mafic-ultramafic belt

The Argentine Precordillera is a fold and thrust belt located in central-western Argentina, within the subhorizontal subduction segment of the Nazca plate (Central Andes) (Fig. 1A).

In particular, its western sector consists of Ordovician-Devonian metasedimentary rocks of slope and deep marine settings, some of which host Cambrian carbonate olistoliths that belonged to a carbonate platform environment, and siliciclastic rocks from its basement (Thomas and Astini, 2003 and others therein). These associations are spatially related to mafic and ultramafic bodies grouped in the Argentine Precordillera mafic-ultramafic belt (Fig. 1B). This belt crops out discontinuously between 28° and 33°SL and consists of serpentinized ultramafic rocks and massive metagabbros, meta-hyaloclastites, metabasaltic dikes/sills and pillow lavas with greenschist facies metamorphism. The latter show an E-MORB signature and positive εNd values (+6 to +9.3) that show its oceanic character (Haller and Ramos, 1984; Kay *et al.*, 1984; Cortés and Kay, 1994; Fauqué and Villar, 2003). Mafic granulites retrograded to greenschist metamorphism are also described (Davis *et al.*, 1999; Boedo *et al.*, 2012). Both metaigneous and metasedimentary rocks record a metamorphic event dated by K-Ar and Ar-Ar methods to Middle Devonian age, interpreted as the collision of the Chilenia terrane against the Gondwana margin (Cucchi, 1971; Buggisch *et al.*, 1994; Davis *et al.*, 1999).

Haller and Ramos (1984) considered that the southernmost part of the mafic-ultramafic belt is exposed in the Guarguaraz area, Frontal Cordillera (Fig. 1B). In this area there are outcrops of serpentinized ultramafic bodies, gabbros, basaltic dikes and pillow lavas associated to marbles, mica schists and quartz schists (Villar, 1969, 1970; Bjerg *et al.*, 1990; Gregori and Bjerg, 1997; Gargiulo *et al.*, 2011, among others). U-Pb ages from zircon show a maximum deposition age of 555±8Ma for these metasediments (Willner *et al.*, 2008), being consistent with findings of probable Vendian-Cambrian cyanobacteria and acritarch fauna and a metabasite with a crystallization age of 655±76Ma (Sm-Nd whole rock) (López de Azarevich *et al.*, 2009). As in the Precordillera, the Guarguaraz mafic bodies have a N- to E-MORB signature and the whole sequence is strongly metamorphosed and deformed. Massonne and Calderón (2008) and Willner *et al.* (2011) estimated anticlockwise P-T paths on metapelites and metabasites yielding high pressure conditions (albite amphibolite facies) followed by a decompression stage, which are compatible with the burial and exhumation of material in a collisional setting. Besides, Willner *et al.* (2011) reported a 390±2Ma age (Lu-Hf on garnet) interpreted as the time of collision of the Chilenia terrane against the Gondwana margin.

There is some consensus that both localities belong to an almost complete ophiolite sequence formed in a mid-ocean ridge, obducted by the collision of the Chilenia terrane against the Gondwana margin during the Middle-Late Devonian (Haller and Ramos, 1984; Ramos *et al.*, 1984, 1986). Based on U-Pb ages and geochemical data, other authors suggest that mafic and ultramafic bodies would have been generated in different tectonic environments including a mid-ocean ridge (for the pillow lavas, mafic dikes/sills and massive gabbros) and the roots of a magmatic arc (for the mafic granulites) (Davis *et al.*, 1999, 2000). In contrast, Loeske (1993) proposed that the belt belongs to the ocean floor of a back-arc basin based on geochemical and detrital sediment studies.

Field occurrence and petrographic features of the Peñasco serpentinites

The study zone is located in the Cordón del Peñasco area, at the northernmost part of the province of Mendoza between 32°6'20'' and 32º14'19''S and 69°9'15'' and 69º3'55''W (Fig. 1B). There deep marine and slope metasedimentary rocks associated with ultramafic rock bodies with advanced to complete serpentinization crop out. In tectonic contact with these bodies are mafic granulites, whose protoliths are layered gabbros since igneous layering is preserved. These bodies are retrograded to greenschist facies metamorphism. In addition, there are basaltic dikes/sills intruding the serpentinites and the metasedimentary successions, assigned to the early Paleozoic and subordinate amygdaloidal metabasites and metahyaloclastites. Both metaigneous and metasedimentary rocks are affected by greenschist facies metamorphism (Harrington, 1971; Boedo *et al.*, 2012; among others).

The serpentinites are widely distributed in the study area, forming north- to northeast-trending west-vergent klippes. They consist of dark to light green, gray-green and black lenticular bodies of variable dimensions (tens to hundreds of meters), with a silky shine and, generally, a massive appearance. Occasionally, stockwork texture is present comprising numerous veinlets and veins a few centimeters to millimeters thick, which are filled with carbonates or serpentines that have grown perpendicularly and/or obliquely to the wall of the veins (Fig. 2A).

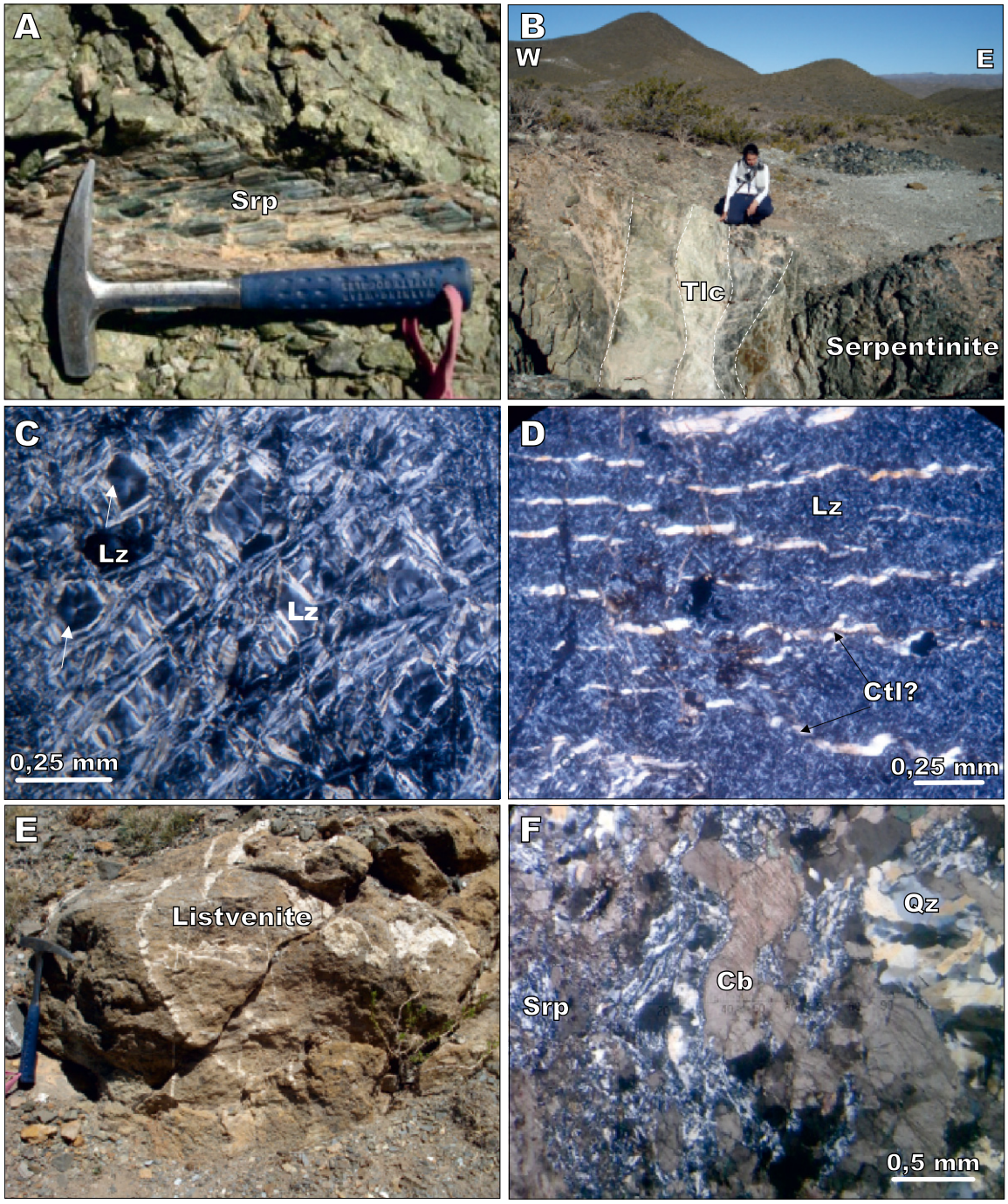

FIGURE 2. A) Peñasco area. Serpentinite vein filled with fibrous serpentine that has grown obliquely to the wall of the vein. B) Peñasco area. View to the south of a contact zone between a serpentinite (to the east) and a metasedimentary country rock (to the west). Reaction zones of different colors tens of centimeters thick develop. C) Microphotograph of a serpentinite with a mesh texture and hourglass texture in its centre (white arrows). D) Microphotograph of a serpentinite with lizardite interpenetrative texture dissected by subparallel veinlets of possible chrysotile. E) Northern Peñasco area. Rusty orange listvenite body dissected by calcite veins and veinlets of a few centimeters thick. F) Microphotograph of a listvenite (silica-carbonate rock) composed of quartz, carbonate and relic serpentines. Mineral symbols used are those proposed by Whitney and Evans (2010).

The contacts between the serpentinites and their country rock (slates, phyllites and subordinate metacarbonates) are strongly sheared. At these boundaries, concentric/subconcentric reaction zones developed around the ultramafic body, with transitional contacts and thicknesses from tens of centimeters to a few meters, and variable colors according to mineral content: white (due to the presence of talc), light green (talc+serpentine), bluish gray and black (serpentine+chlorite) (Fig. 2B). Euhedral crystals of pyrite in talc schists are also observed. In many

cases, rusty orange listvenites up to 50 meters wide are associated with serpentinite margins near tectonic contacts with the Peñasco metasedimentary rocks. They consist of quartz, carbonate, chlorite, Fe oxides, relict serpentines and Cr-spinels. As these bodies are associated with major faults whereas intermediate to acidic plutons are relatively far from these rock bodies (up to 100km), we discard an origin related to andesitic-granitic plutons.

Under the microscope serpentinization is advanced to complete with pseudomorphic/non-pseudomorphic replacement textures, and serpentine veinlets (Figs. 2C–E). Anhedral reddish-brown Cr-spinels and scarce pentlandite and Co-pentlandite constitute the only relict phases. Lizardite mesh with hourglass texture (Fig. 2C) or interpenetrative/cryptocrystalline-interpenetrative texture can be recognized, dissected by veins and veinlets whose thickness varies from <0.1 to 1mm (Fig. 2D). Moreover, blasts of clinochrysotile, magnetite, chlorite, brucite and anhedral crystals of Cr-spinel with chlorite growing at their expense are present (Fig. 2E). In some cases, samples with stockwork textures exhibit up to four generations of veins (Fig. 2E). Occasionally, where serpentinization is not complete, magnetite and serpentine were recognized along cleavage planes of relict orthopyroxene. Many samples exhibit carbonate patches associated with serpentine and quartz, which manifest the process of listvenitization (Fig. 2F), best developed at the margins of the serpentinite bodies.

MATERIALS AND METHODS

We collected 11 representative samples of serpentinized ultramafic rocks from the Argentine Precordillera mafic-ultramafic belt found at the Peñasco, Pozos, Cortaderas and Bonilla localities (Table 1). Eight samples were taken from the Cordón del Peñasco, while the remaining were taken from Pozos, Cortaderas and Bonilla areas (Fig. 1B). We use here the term "serpentinite" to define ultrabasic rock bodies where the serpentinization process is advanced or complete, such that there are no relics of primary assemblages or original rock textures, and "listvenite" as a silica-carbonate rock product of low-grade metasomatic processes after ultramafic rocks.

The samples were prepared and analyzed following standard procedures. They were milled with a jaw crusher and an agate mortar at the Institute of Geochronology and Isotope Geology (INGEIS) from the Universidad de Buenos Aires-CONICET. Only pieces of the sample which appeared vein-free were used. The samples were analyzed at ACTLABS Laboratories (Canada) where they were prepared and analyzed in a batch system. Each batch contains a method reagent blank, certified reference material and 17% replicates. Samples were mixed with a flux of lithium metaborate and lithium tetraborate and fused in an induction furnace. The molten melt was poured into a solution of 5% nitric acid containing an internal standard, and mixed until completely dissolved. Samples were run for major oxides and selected trace elements (Ba, Be, Sc, Sr, V, Y, Zr) on an ICP (detection limit: 0.01%, MnO and TiO2: 0.001%). Trace elements were measured by Inductively Coupled Plasma Mass Spectrometry (ICP-MS). Results are shown in Table 1, major and trace element concentrations are in weight percent (wt%) and parts per million (ppm), respectively.

The composition of spinel group minerals were analyzed with a JEOL JXA-8230 electron microprobe at the Laboratorio de Microscopía Electrónica y Análisis por Rayos X (LAMARX) of the Universidad Nacional de Córdoba, Argentina. For full quantitative analysis, four wavelength-dispersive spectrometers (WDS) were used. Operating conditions were an acceleration voltage of 15kV for a beam diameter of about 1μm and a beam current of 20nA. Concentrations of Si, Al, Ti, Ca, Mg, Fe, Mn, Na, Cr, V and Zn were determined. Standards were natural minerals: chromite for Mg, Cr and Al; ilmenite for Ti and Fe^{2+}; rhodonite for Mn; vanadinite for V; nickeline for Ni; fayalite for Si; anorthoclase for Na; zoisite for Ca and gahnite for Zn. Results are presented in Table 2. Fe^{3+} contents were estimated by the method proposed by Droop (1987).

In order to determine the type of serpentine present, X-ray diffraction studies were performed at Universidad Nacional de Córdoba with a difractometer Rigaku D-Max IIC. Operating conditions were: 5–70° 2θ, velocity 3°/minute, step 0.02, radiation Cu (Kα=1.5405A). Software employed was MDI Jade 7.

RESULTS AND DISCUSSION

Composition of relict Cr-spinel

Cr-spinels can be recognized by their intercumulus relic disposition (Fig. 3A) or by their holly leaf shapes (Fig. 3B). Their rims are usually altered to ferritchromite, magnetite or Cr-rich magnetite (Fig. 3C), but occasionally the whole crystal is altered showing spongy appearance (Fig. 3D).

Fresh crystals are unzoned (Fig. 3C) and exhibit an homogeneous composition, with Cr# (=Cr/(Cr+Al) atomic ratio) between 0.35 and 0.50 and Mg# (=Mg/(Mg+Fe^{2+}) atomic ratio) between 0.56–0.72. MnO, V_2O_3 and ZnO do not exceed 0.4%. Chromites from sample LJ 22-12 show high TiO_2 contents between 0.4–0.5% and restricted Al_2O_3

TABLE 1. Chemical data set of the Peñasco serpentinites. Major and trace element contents are given in wt% and ppm, respectively

Locality	Northern Cordón del Peñasco			Central Cordón del Peñasco					Pozos area	Bonilla area	Cortaderas area
Sample	EN 1-12	EN 3-12	EN 12-12	LJ 21-12	QM 7-08	QM 8-08	QM 28-08	QM 38-08	QP 7	SE 15A	M1
SiO_2	39,83	38,63	40,17	38,37	39,22	34,12	40,28	40,74	38,27	40,40	39,88
TiO_2	b.d.l[1]	0,04	0,02	0,01	0,01	0,01	0,06	0,01	0,02	0,07	0,02
Al_2O_3	0,72	1,76	1,47	1,86	0,65	0,62	1,88	0,35	1,95	2,30	1,08
Fe_2O_3T	5,64	6,01	5,51	6,63	6,78	6,28	5,42	6,95	6,32	6,19	5,98
MnO	0,05	0,11	0,08	0,09	0,09	0,10	0,10	0,08	0,12	0,09	0,08
MgO	36,21	37,14	37,40	36,67	35,22	30,78	36,31	36,65	36,14	36,73	36,29
CaO	1,18	0,11	0,34	0,08	2,94	10,60	0,77	0,12	0,19	0,06	1,46
Na_2O	0,01	b.d.l	0,02	b.d.l	0,02	0,03	0,02	0,01	b.d.l	b.d.l	b.d.l
K_2O	b.d.l	b.d.l	b.d.l	b.d.l	0,01	0,01	b.d.l	b.d.l	b.d.l	b.d.l	b.d.l
P_2O_5	b.d.l	0,02	b.d.l	b.d.l	b.d.l	b.d.l	b.d.l	b.d.l	b.d.l	b.d.l	b.d.l
LOI	15,53	13,38	13,67	13,16	14,44	17,71	13,98	12,10	13,56	12,14	12,41
Total	99,16	97,20	98,68	96,87	99,37	100,30	98,81	97,00	96,56	97,97	97,20
La	8,25	9,00	3,80	3,89	0,17	0,19	3,18	3,81	8,73	3,50	6,38
Ce	11,80	14,30	4,37	4,20	0,42	0,41	4,72	5,32	12,80	4,49	10,40
Pr	1,48	1,71	0,53	0,77	0,04	0,05	0,62	2,05	1,40	0,67	1,21
Nd	4,38	5,73	1,60	2,16	0,13	0,14	1,72	2,13	3,70	2,16	3,80
Pm	-	-	-	-			-	-	-	-	-
Sm	0,72	0,94	0,30	0,49	0,01	0,01	0,32	0,38	0,40	0,31	0,59
Eu	0,21	0,30	0,15	0,13	0,02	0,05	0,15	0,36	0,71	0,33	0,14
Gd	0,30	0,58	0,14	0,18	0,03	0,02	0,21	0,17	0,21	0,25	0,31
Tb	0,04	0,09	0,03	0,03	b.d.l	b.d.l	0,04	0,03	0,04	0,04	0,04
Dy	0,18	0,45	0,18	0,18	0,04	0,03	0,22	0,15	0,23	0,23	0,18
Ho	0,03	0,08	0,04	0,04	b.d.l	b.d.l	0,04	0,03	0,05	0,05	0,03
Er	0,09	0,22	0,13	0,11	0,03	0,01	0,14	0,09	0,15	0,15	0,09
Tm	0,01	0,03	0,02	0,02	b.d.l	b.d.l	0,02	0,01	0,03	0,03	0,02
Yb	0,10	0,20	0,14	0,12	0,03	0,01	0,16	0,10	0,20	0,19	0,13
Lu	0,02	0,03	0,02	0,02	0	b.d.l	0,03	0,02	0,04	0,04	0,03
Sr	33	8	8	4	24	67	16	3	4	3	20
Ba	7	6	7	b.d.l	7	9	8	3	6	b.d.l	b.d.l
Cs	0,50	b.d.l	b.d.l	b.d.l	b.d.l	b.d.l	b.d.l	b.d.l	b.d.l	b.d.l	b.d.l
Rb	b.d.l	b.d.l	b.d.l	b.d.l	b.d.l	b.d.l	b.d.l	b.d.l	b.d.l	b.d.l	b.d.l
U	0,99	0,09	0,27	0,16	1	2	0,14	1,39	0,23	0,05	b.d.l
Th	0,49	0,65	0,16	0,19	0	b.d.l	0,23	0,23	0,50	0,19	0,42
Hf	b.d.l	b.d.l	b.d.l	b.d.l	b.d.l	b.d.l	b.d.l	b.d.l	b.d.l	b.d.l	b.d.l
Nb	b.d.l	0,6	b.d.l	b.d.l	b.d.l	b.d.l	b.d.l	b.d.l	b.d.l	b.d.l	b.d.l
Ta	0,19	b.d.l	b.d.l	b.d.l	b.d.l	b.d.l	0,02	b.d.l	b.d.l	b.d.l	b.d.l
Sc	6	9	8	9	6	4	10	3	11	11	6
Cr	2280	2480	2310	2200	2460	2340	2650	2210	2670	2200	2070
Ni	2080	2130	2160	2040	2400	1690	1970	1990	2060	1830	1970
Co	99	107	102	104	105	75	88	93	103	91	105
Pb	b.d.l	b.d.l	b.d.l	b.d.l	b.d.l	b.d.l	b.d.l	b.d.l	b.d.l	b.d.l	b.d.l
Nb	b.d.l	0,60	b.d.l	b.d.l	b.d.l	b.d.l	b.d.l	b.d.l	b.d.l	b.d.l	b.d.l
Zr	b.d.l	2	b.d.l	b.d.l	2	b.d.l	2	b.d.l	b.d.l	1	b.d.l
V	22	49	40	39	25	25	53	25	57	62	37
Y	b.d.l	2,00	0,90	1,00	b.d.l	b.d.l	1,00	b.d.l	1,20	1,00	0,70

[1]b.d.l: below detection limit

TABLE 2. Chemical data set of the Cr-spinel group minerals from the Peñasco serpentinites. Element contents are given in wt%

Sample	EN 16-12										LJ 21-12				LJ 22-12				
SiO_2	-	-	-	-	-	-	-	-	-	-	-	-	0,12	-	-	-	-	-	-
TiO_2	0,11	0,12	0,07	0,13	0,10	0,09	0,06	0,09	0,09	0,09	0,05	0,04	0,05	0,08	0,48	0,47	0,45	0,41	0,51
Al_2O_3	32,71	30,59	33,49	32,39	37,20	37,65	36,83	36,47	35,84	34,04	36,33	33,99	27,39	28,79	30,73	30,84	30,80	29,91	29,87
Cr_2O_3	35,12	38,16	35,05	33,73	30,02	29,98	30,74	31,24	32,34	34,60	30,99	33,78	36,91	36,45	33,46	33,16	33,61	33,04	33,44
NiO	0,08	-	0,16	0,12	0,16	0,10	0,14	0,16	0,08	0,14	0,18	0,13	0,08	0,03	0,12	0,10	0,05	0,15	0,12
V_2O_3	0,05	0,25	0,07	0,13	0,22	0,16	0,16	0,21	0,14	0,18	0,13	0,16	0,20	0,18	0,16	0,15	0,21	0,29	0,22
FeO	15,48	15,89	15,71	16,23	15,20	14,88	15,26	14,89	14,03	15,09	14,85	15,76	18,63	18,15	18,54	18,52	19,30	18,59	19,38
MgO	15,53	15,40	16,11	14,80	16,29	16,53	16,44	16,37	16,68	16,77	17,29	16,44	13,54	14,09	14,93	14,95	15,32	14,57	14,69
MnO	0,27	0,23	0,24	0,27	0,23	0,23	0,18	0,23	0,24	0,27	0,33	0,24	0,35	0,27	0,27	0,23	0,27	0,27	0,27
CaO	-	-	-	-	-	-	0,03	-	-	-	-	-	0,02	-	-	-	-	-	-
ZnO	0,25	0,13	0,26	0,10	0,19	0,23	0,20	0,21	0,13	0,22	0,28	0,10	0,28	0,19	0,18	0,17	0,12	0,10	0,16
Na_2O	0,01	-	0,02	0,01	0,02	-	0,03	-	-	-	-	-	-	-	-	-	-	-	-
Total	99,43	100,57	101,05	97,81	99,52	99,66	99,96	99,71	99,39	101,23	100,29	100,46	97,57	98,03	98,87	98,58	100,13	97,32	98,66
Si	-	-	-	-	-	-	-	-	-	-	-	-	-	-	-	-	-	-	-
Ti	0,002	0,003	0,002	0,003	0,002	0,002	0,001	0,002	0,002	0,002	0,001	0,001	0,001	0,002	0,011	0,011	0,010	0,010	0,012
Al	1,135	1,060	1,141	1,144	1,261	1,271	1,246	1,237	1,219	1,152	1,225	1,160	1,000	1,039	1,104	1,109	1,094	1,094	1,081
Cr	0,817	0,887	0,801	0,799	0,683	0,679	0,698	0,711	0,738	0,785	0,701	0,773	0,904	0,882	0,806	0,800	0,801	0,811	0,812
Ni	0,002	-	0,004	0,003	0,004	0,002	0,003	0,004	0,002	0,003	0,004	0,003	0,002	0,001	0,003	0,002	0,001	0,004	0,003
V	0,001	0,006	0,002	0,003	0,005	0,004	0,004	0,005	0,003	0,004	0,003	0,004	0,005	0,004	0,004	0,004	0,005	0,007	0,005
Fe^{2+}	0,381	0,391	0,380	0,407	0,366	0,357	0,366	0,359	0,338	0,362	0,355	0,382	0,483	0,465	0,425	0,425	0,438	0,434	0,448
Mg	0,681	0,675	0,694	0,661	0,699	0,706	0,703	0,703	0,717	0,717	0,737	0,710	0,626	0,643	0,678	0,680	0,688	0,674	0,672
Mn	0,007	0,006	0,006	0,007	0,006	0,006	0,004	0,006	0,006	0,007	0,008	0,006	0,009	0,007	0,007	0,006	0,007	0,007	0,007
Ca	-	-	-	-	-	-	0,001	-	-	-	-	-	0,001	-	-	-	-	-	-
Zn	0,006	0,003	0,006	0,002	0,004	0,005	0,004	0,005	0,003	0,005	0,006	0,002	0,006	0,004	0,004	0,004	0,003	0,002	0,004
Na	0,001	-	0,001	0,001	0,001	-	0,002	-	-	-	-	-	-	-	-	-	-	-	-
Fe^{3+}	0,07	0,06	0,08	0,07	0,07	0,07	0,08	0,07	0,06	0,08	0,10	0,09	0,11	0,11	0,10	0,10	0,11	0,10	0,11
Cr#	0,42	0,46	0,41	0,41	0,35	0,35	0,36	0,36	0,38	0,41	0,36	0,40	0,47	0,46	0,42	0,42	0,42	0,43	0,43
Mg#	0,64	0,63	0,65	0,62	0,66	0,66	0,66	0,66	0,68	0,66	0,67	0,65	0,56	0,58	0,61	0,62	0,61	0,61	0,60

concentrations, whereas chromites from the remaining samples (EN 1-12, 16-12 and LJ 21-12) are poorer in TiO_2 (up to 0.1%) and richer in Al_2O_3 and Cr_2O_3 (Fig. 4A–C). Chromites from sample EN 1-12 exhibit the highest Cr_2O_3 and MgO values (Fig. 4D).

Unusual compositions can be attributed to metasomatism (Mukherjee *et al.*, 2010; Singh and Singh, 2013, among others) and can be separated in two groups: 1) MnO–ZnO rich and MgO–Al_2O_3 poor crystals, and 2) MnO rich and Al_2O_3-Cr_2O_3 poor crystals. The first group shows MnO contents up to 9.6% and ZnO concentrations that occasionally exceed 1.5%. Al_2O_3 does not exceed 3% and MgO contents reach 5%. The second group exhibits MnO contents of 3.5–4.7%, with Al_2O_3 and Cr_2O_3 concentrations up to 6.7% and 17.8%, respectively. The presence of frequent silicate microinclusions are shown by high SiO_2 contents (up to 20%, analyses not included) in Cr-spinel analyses.

Spinels are classified as picotites and pleonaste and, to a lesser extent, spinel *sensu stricto* (Fig. 5) according to the chemical variation of spinels (solid solution spinel-hercynite-chromite-magnesiochromite-magnesioferrite-magnetite).

Cr-rich spinels are good petrogenetic indicators of mafic-ultramafic rocks. In particular, Cr# rarely exceed 0.6 in Mid-Ocean-Ridge (MOR) rocks (0.2–0.6 according to Haggerty, 1991), whereas arc rocks can reach values of 0.9, and intraplate settings influenced by mantle plumes have >0.7 (Haggerty, 1991). It is broadly accepted that Cr# values >0.6 reflect high degree of melting (Dick and Bullen, 1984; Arai *et al.*, 2011), so mid-ocean-ridge ultramafic rocks will exhibit Cr# between 0.2 and 0.6 (Coish and Gardner, 2004; Deschamps *et al.*, 2013). Cr# and TiO_2 spinel contents suggest that the majority of the Peñasco serpentinites experienced a significant degree of partial melting (>20%) (Fig. 6A). Cr-spinels from sample LJ 22-12 lie in a melt-mantle interaction trend similar to the one described by Pearce *et al.* (2000) for the South Sandwich trench-fracture zone intersection peridotites. This sample could have originated from an interaction between a MORB-like melt and a mantle that had experienced relatively little partial melting (up to 10%). From Cr# versus Mg# diagram, there is no obvious discrimination since samples plot in the superposition zone of Forearc, Backarc and Abbysal peridotite settings (Fig. 6B). In accordance, on the TiO_2 versus Al_2O_3 diagram (Kamenetsky *et al.*, 2001), the Peñasco Cr-spinels plot within the fields of the MORB and suprasudbudction zone (SSZ) peridotites (Fig. 6C), whereas on the Cr# versus $Fe^{2+}/(Mg^{+}Fe^{2+})$ diagram, samples plot within the array of ocean floor peridotites (Fig. 6D) and follow the Ca-Al trend proposed by Barnes and Roeder (2001). This trend shows a widely variable Cr# at generally low $Fe^{2+}/(Mg^{+}Fe^{2+})$. It

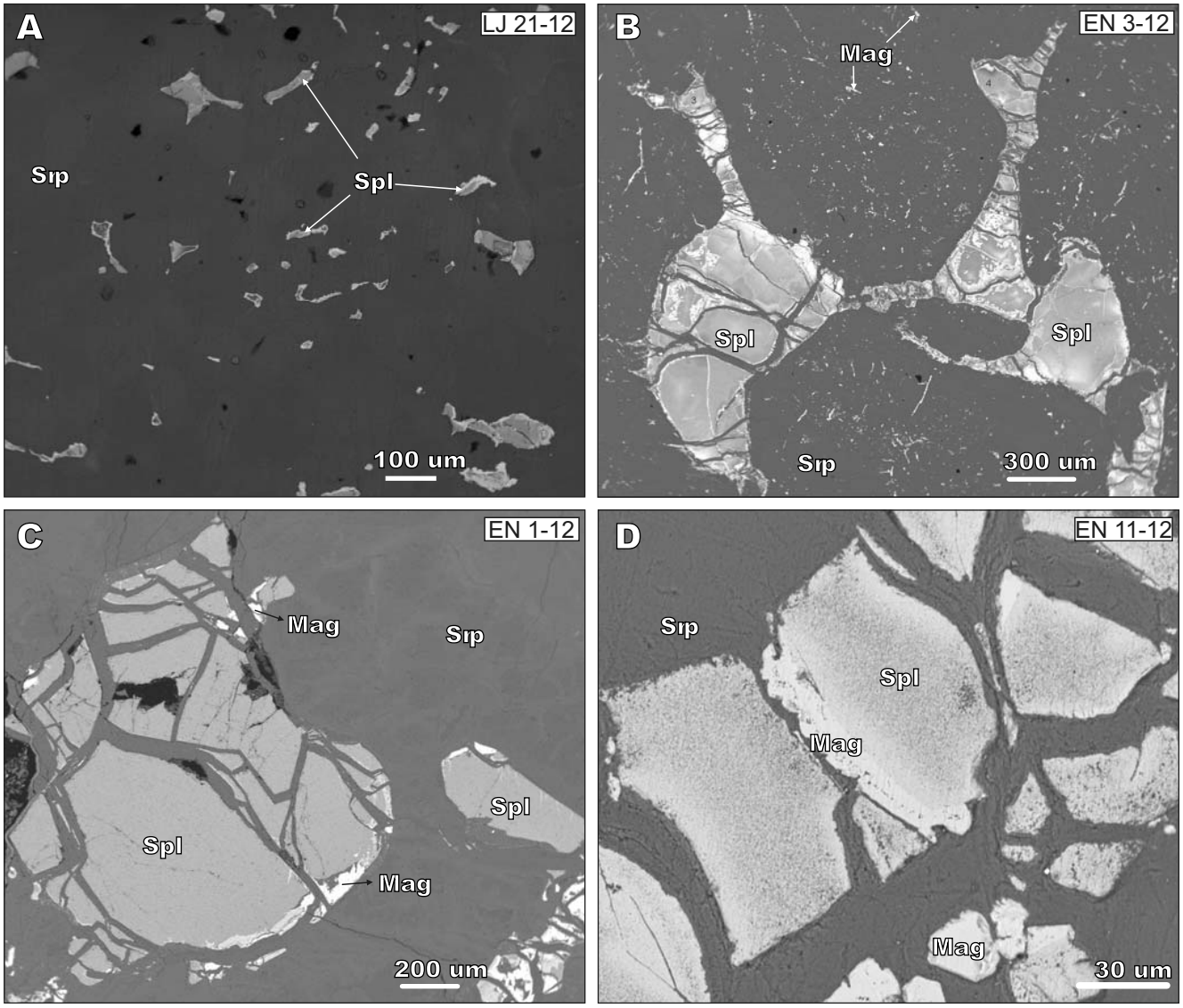

FIGURE 3. A) Back scattered electron (BSE) image of a serpentinite with relict intercumulus Cr-spinels. B) BSE image of a serpentinite with metasomatized Cr-spinels showing holly leaf shapes. C) BSE image of chemically homogeneous Cr-spinels with a thin rim of magnetite. D) BSE image of a Cr-spinel almost completely altered to magnetite. Mineral symbols used are those proposed by Whitney and Evans (2010).

was first described by Irvine (1967), who explained that it corresponds to spinels equilibrating with olivine at constant composition and temperature. It is particularly evident in the various mantle and lower-crustal samples such as xenoliths, ophiolites and ocean-floor peridotites (Barnes and Roeder, 2001). From Cr-spinel chemistry, the Peñasco serpentinites exhibit an intermediate signature between MOR and arc-related settings.

Geochemical aspects of the Peñasco serpentinites

The whole rock analyses show that the Peñasco samples have SiO_2 concentrations that vary over a small range (45.8–47.9wt%), with Al_2O_3 between 0.4 and 2.6wt% and Mg# varies from 0.93 to 0.94 (MgO varying between 42.8 and 44.3wt%). Samples reach TiO_2 concentrations up to 0.07wt% and CaO values do not exceed 2.9wt%. Some samples analyzed show addition of CaO up to 10wt% (Table 1), which evidence the carbonatization. Loss on ignition (LOI) values are high (12.1–17.7%), which could be considered as a parameter of the advanced to complete serpentinization process. However, some authors suggest that, among serpentines, carbonates and other hydrous minerals such as brucite could influence these values (Deschamps *et al.*, 2013). Surely, the latter is the case for several of the studied samples since pure serpentinite has 13wt% H_2O.

Cr and Ni contents are between 2070–2650ppm and 1690–2400ppm, respectively. Co concentrations range

from 75 to 107ppm, whereas V contents vary between 22 and 62ppm. We interpret a cumulate origin for the Peñasco serpentinites since these values are similar to those informed by Coleman (1977) for ophiolite ultramafic cumulates. In general, when normalized to chondrite CI (Sun and McDonough, 1989), serpentinites show enriched REE patterns up to 40 times higher than the chondritic values, with an evident relative Light Rare Earth Elements (LREE) enrichment over Heavy Rare Earth Elements (HREE) ($(La/Yb)_{CN}$=13-59), and marked positive Eu anomalies (Eu/Eu* up to 7.5, being $Eu^*=(Sm_N x Gd_N)^{1/2}$ –Taylor and McLennan, 1985) (Fig. 7A). In particular, there is a LREE fractionation with $(La/Sm)_{CN}$ values between 5.1 and 14, while HREE have subhorizontal to slightly positive slopes ($(Sm/Yb)_{CN}$: 1.8-8), which indicate that protoliths were at a mantle depth out of the garnet stability field.

Serpentinites exhibit Th and U (and occasionally Cs) enrichment and negative anomaly on HFSE such as Zr and Ti (Fig. 7B). U enrichments and Cs erratic values can be explained by weathering processes occurring near the seafloor (Kodolànyi *et al.*, 2012 and others mentioned therein).

Neither the high REE contents nor the positive Eu anomalies (Figs. 7A) could have been inherited from the original ultramafic mineral assemblage, since olivine and pyroxene are not important REE carriers and there is no evidence of relict plagioclase or mantle refertilization. Some samples also exhibit moderate Sr concentrations, which are affected by serpentinization or carbonatization. In carbonate-bearing serpentinites, carbonates are the most important Sr carriers (between 1 and 2 orders of magnitude higher than in serpentine), while in carbonate-free serpentinites, serpentines are the main Sr carriers (Kodolànyi *et al.*, 2012). In the examined serpentinites the amount of carbonate increase toward the margins, where listvenites can be found. It is noteworthy that despite the fact that all analyzed serpentinites show the same REE enriched patterns, not all of them contain carbonates in hand specimen or in thin section. In some cases, the only

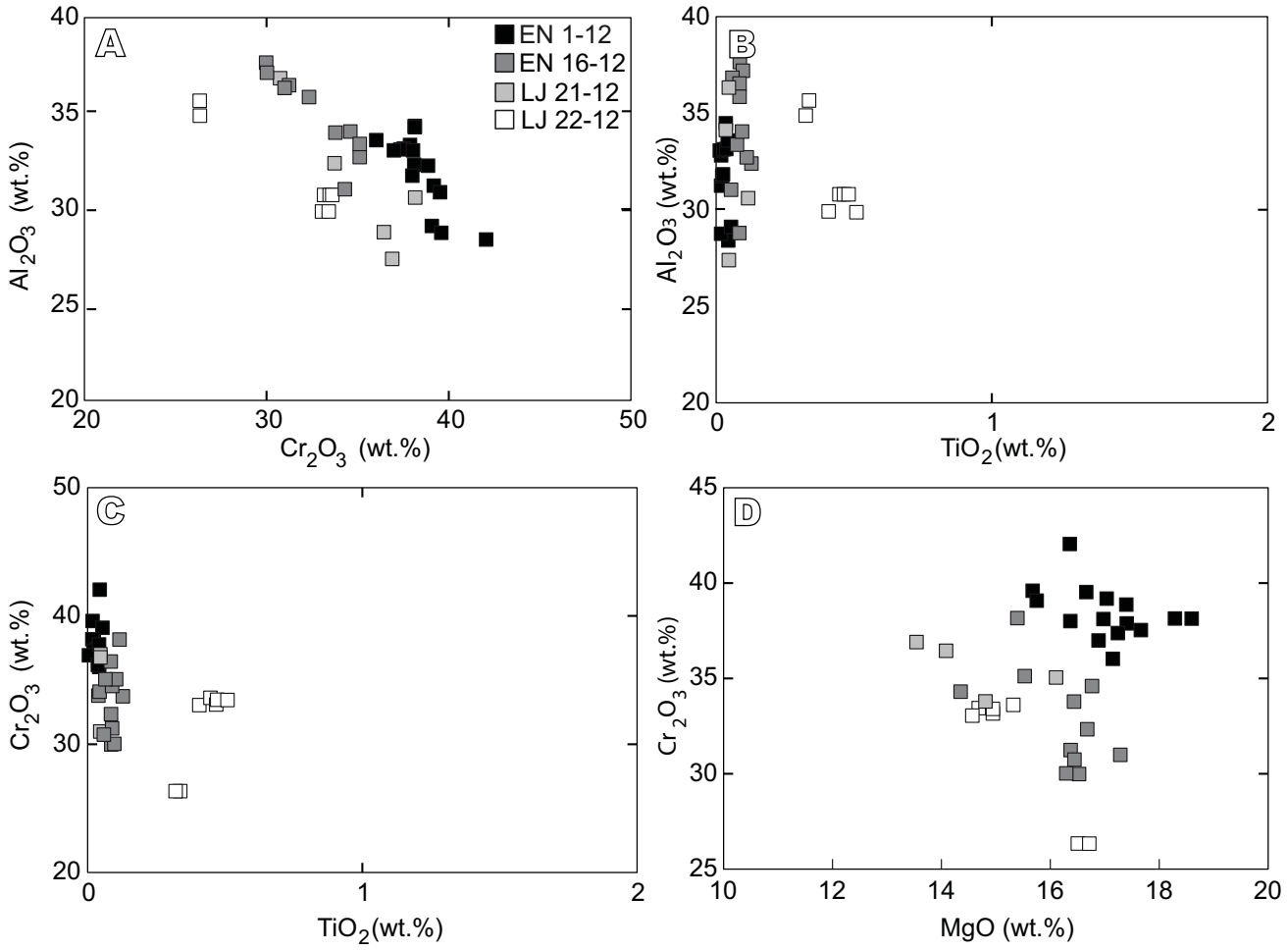

FIGURE 4. A) Al_2O_3 versus Cr_2O_3 diagram showing trends of analyzed Cr-spinels from different serpentinite samples. B) Al_2O_3 versus TiO_2 diagram. C) Cr_2O_3 versus TiO_2 diagram. D) Cr_2O_3 versus MgO diagram. Oxides are expressed in weight percent (wt%).

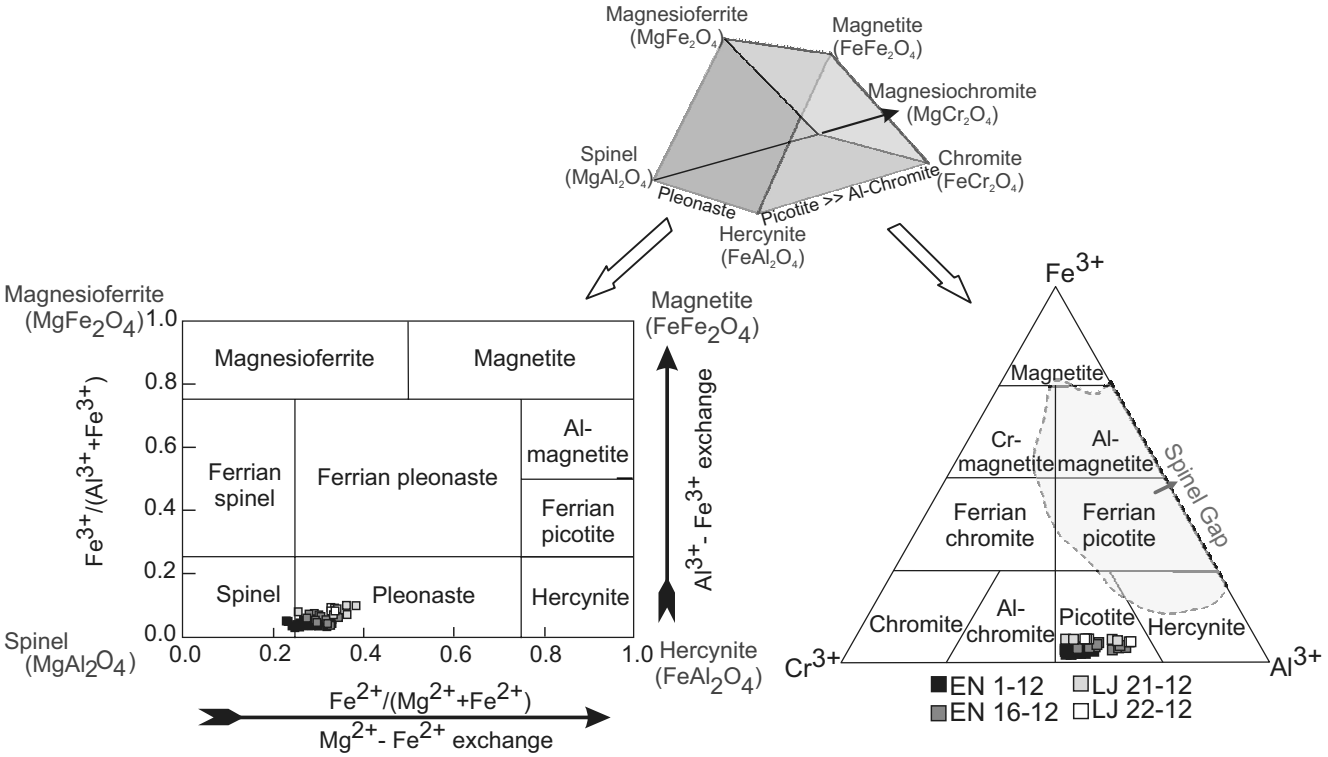

FIGURE 5. Chemical classification diagrams for the spinel group minerals of the Peñasco area. Spinel prism for the multi-component system: spinel-hercynite-chromite-magnesiochromite-magnesioferrite-magnetite. Binary classification diagram considering the Mg^{2+}-Fe^{2+} and Al^{3+}-Fe^{3+} exchanges (left). Triangular classification diagram Cr^{3+}-Fe^{3+}-Al^{3+}. Spinel gap field from Barnes and Roeder (2001) (right). Diagrams taken from Gargiulo *et al.* (2013).

evidence for metasomatism are chemically altered relict Cr-spinels (discussed above). Hence, the metasomatism in some serpentinites could be cryptic as well.

Hydrothermal alteration and listvenitization

From their original setting through their tectonic emplacement in metasediments, the Peñasco serpentinite bodies exhibit a complex history of alteration and metasomatism. At first, the ultramafic bodies were affected by serpentinization under low pressure and temperature conditions (hydrothermal alteration of ocean floor) mainly evidenced by the presence of lizardite and chrysotile forming pseudomorphic textures after olivine (mesh and hourglass textures). The recognized assemblage lizardite+chrysotile+magnetite±brucite±chlorite indicates that the maximum temperature reached during ocean-floor alteration was ≤300ºC (Evans, 1977, 2004).

Ideally, serpentinites can be described as a series of minerals with compositions essentially on a tie-line between $Mg(OH)_2$ (brucite) and $Mg_3Si_4O_{10}(OH)_2$ (talc) in the system MgO-SiO_2-H_2O (MSH) (Mellini *et al.*, 1987). At low temperature conditions (<300ºC), serpentinites consist mainly of lizardite and chrysotile (Evans, 1977, 2004). Both minerals are replaced by antigorite during prograde metamorphism. Antigorite stability field ranges from >300ºC to 600–640ºC, which constitute a temperature range of 300ºC or more (Wunder *et al.*, 2001; Bromiley and Pawley, 2003).

From petrographic and geochemical features already described and parageneses defined by Evans (1977, 2004), Winkler (1978) and Spear (1995), the Peñasco serpentinites are considered in the MgO-SiO_2-H_2O-Al_2O_3-FeO (MSHAF) system and are characterized by high initial Fo/En and affected by greenschist facies metamorphism. Occasionally, chlorite (aluminous phase) occurs at Cr-spinel margins and might have gained aluminum during its magnetization.

We do not reject the presence of antigorite in samples not analyzed by X-ray diffraction. From microprobe analyses, we have detected some serpentine patches with SiO_2 contents similar to those of antigorite crystals compiled by Deer *et al.* (1962). If antigorite were formed during low-grade metamorphism, the assemblage antigorite+brucite would suggest temperatures up to 400ºC, in accordance with the chemistry of metasomatic fluids already discussed. We also infer that the fluids involved in the metamorphic event would have had low XCO_2 because if XCO_2 were >10%, serpentines would become unstable (Winkler, 1978).

REE mobilization, Eu positive anomalies, Ca and Sr addition and the presence of carbonate patches can be related to a hydrothermal fluid/serpentinite interaction, with high fluid/rock ratios (>100), at temperatures below 400ºC, as has been interpreted by Menzies *et al.* (1993), Allen and Seyfried (2005) and Paulick *et al.* (2006). Fluids rich in CO_2 and complexing ions such as F^-, Cl^-, PO_4^{3-}, CO_3^{2-}, SO_4^{2-}, among others, coupled with low pH promote REE mobilization (Wood, 1990). During cooling, calcite is known to preferentially incorporate LREE due to the fact that the difference in ionic radius is smaller between Ca and LREE than between Ca and HREE. The marked positive Eu anomalies observed could be related to the presence of Eu as Eu^{2+}, which is easily exchanged with Ca. The presence of abundant carbonate in some samples and the LREE fractionation relative to the HREE suggest an important contribution of CO_3^{2-} ions, which fractionate LREE relative to HREE, implying mildly basic (higher pH) conditions for REE-carbonate complexation (Tsikouras *et al.*, 2006).

The chemistry of the fluid described above is consistent with the absence of silica in serpentinites, which indicates higher pH and moderate to high temperature fluid (350º–400ºC), that holds silica in solution and favors carbonate precipitation (Uçurum, 2000). Overall, the

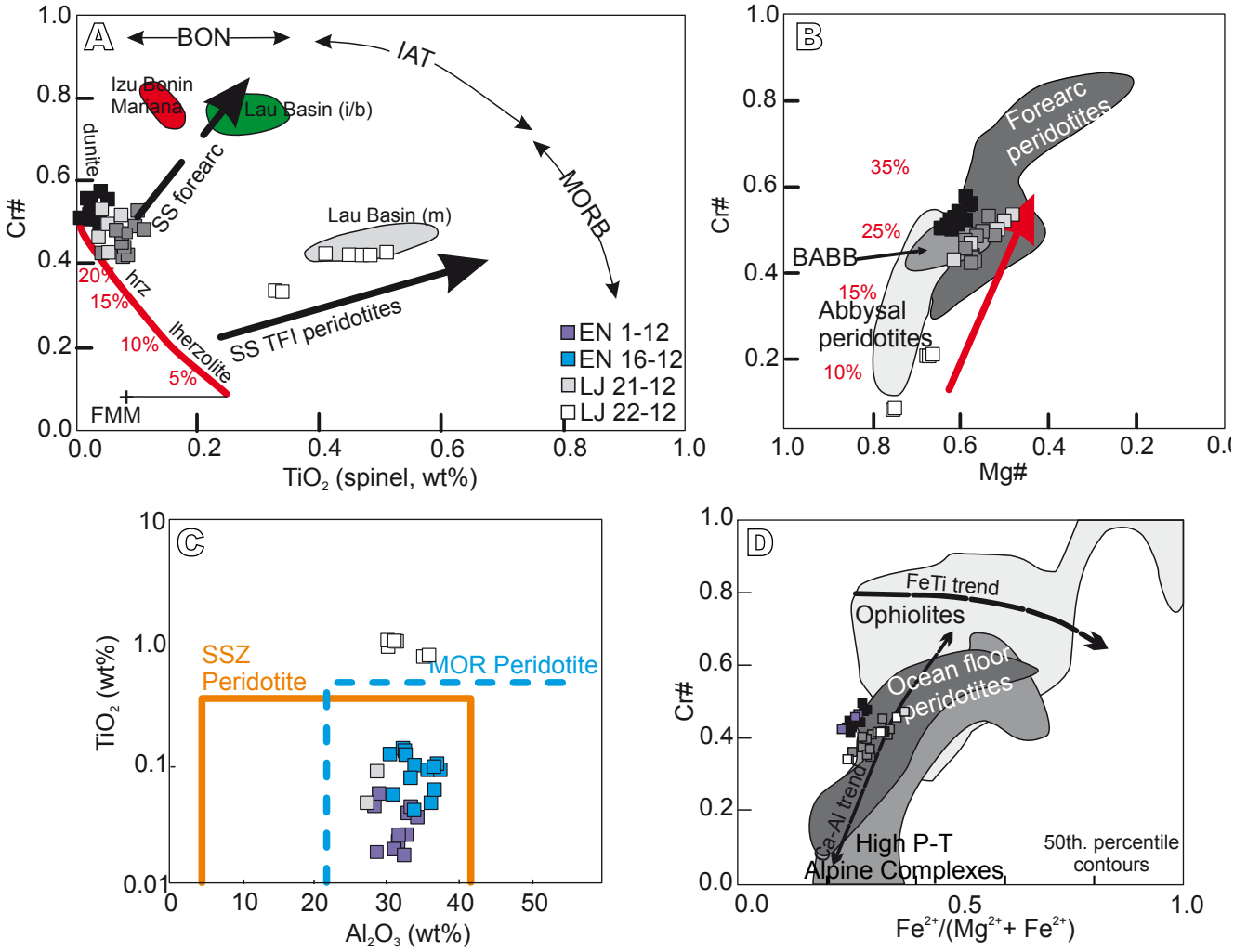

FIGURE 6. Tectonic discrimination diagrams for spinel group minerals from the Peñasco serpentinites. A) $Cr\#^{spl}$ versus TiO_2 (spl, wt%) diagram that discriminates between ultramafic rocks that were affected only by partial melting and those which also experienced melt-mantle interaction. Analyzed Cr-spinels show that samples EN 1-12, EN 16-12 and LJ 21-12 experienced significant partial melting (>20%), whereas sample LJ 22-12 could have been originated by an interaction between a MORB-like melt and a mantle that had experienced relatively little partial melting (10-15%), since its trend is similar to that described by Pearce *et al.* (2000) for the South Sandwich Trench-Fracture Intersection zone peridotites. From Pearce *et al.* (2000). B) $Cr\#^{spl}$ versus $Mg\#^{spl}$ diagram, where forearc, backarc and abyssal peridotites are represented. Except for LJ 22-12, analyzed Cr-spinels plot in the superposition zone of the aforementioned fields. BABB: Back-Arc Basin Basalts. C) TiO_2 (spl, wt%) versus Al_2O_3 (spl, wt%) diagram (from Kamenetsky *et al.*, 2001). Al_2O_3 values >20% imply high degrees of mantle melting and are typical of spinels from mid-ocean ridge peridotites. Cr-spinels from the Peñasco serpentinites plot within the superposition field of mid-ocean ridge (MOR) and suprasubduction zone (SSZ) peridotites. D) C#r versus $Fe^{2+}/(Mg+Fe^{2+})$ diagram. Analyzed Cr-spinels plot within the Ocean Floor Peridotites and follow the Ca-Al trend described by Barnes and Roeder (2001).

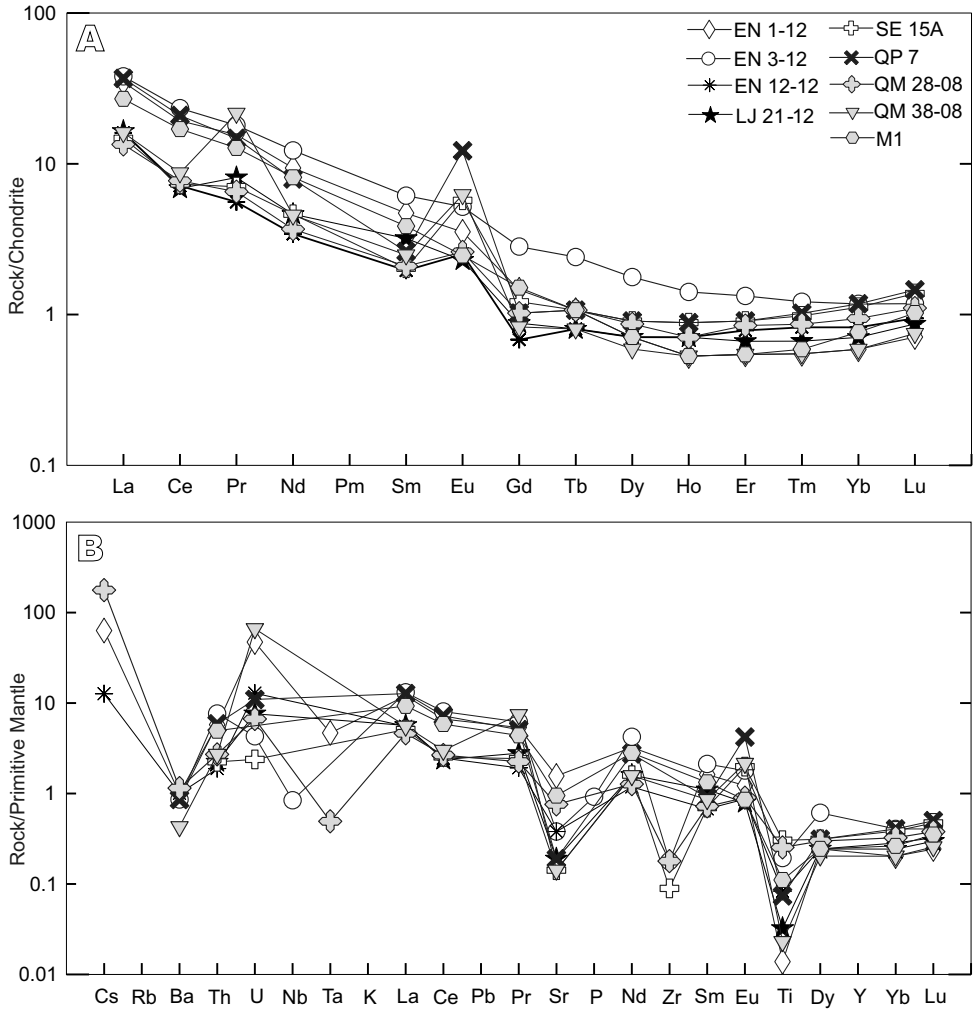

FIGURE 7. A) Chondrite-normalized (Sun and McDonough, 1989) REE diagram for the Peñasco serpentinites. B) Primitive mantle normalized (Sun and McDonough, 1989) trace element diagram.

fluid involved in the metasomatism of serpentinites was a moderate to high temperature (350º–400ºC), CO_2-rich, mildly basic hydrothermal fluid related to the addition of Ca and Sr as has been interpreted by Akbulut *et al*. (2006) for serpentinites from the Mihalıççık region (Turkey). Seawater could be a possible source for CO_2, Ca and Sr. Nevertheless, the presence of listvenites bodies at serpentinite margins with quartz, serpentines, calcite as typical mineral assemblage suggests a multistage fluid influx, where a second type of fluid, which lead at least to quartz precipitation at serpentinite margins, also intervened. Akbulut *et al*. (2006) and Tsikouras *et al*. (2006) describe that the influx of SiO_2 can be driven by low-temperature (<250ºC), highly-oxidized (high fO_2), highly-acid (low pH), saline-rich fluids. The high fO_2 and fS_2 at decreasing temperatures also promotes the precipitation of magnetite and pyrite. Taking into account other examples throughout the world, the high rate of element mobilization during metasomatism should highlight the Precordillera listvenites as potential target for metallic mineralization.

Comparative stratigraphy

The most accepted tectonic evolution of the Cuyania terrane initiates with rifting from Laurentia (Ouachita embayment) in the Neoproterozoic–early Cambrian, and continues with the development of a passive margin in latest early Cambrian to Early Ordovician, and collision with the Gondwana margin in the Middle–Late Ordovician (Astini *et al*., 1995; Naipauer *et al*., 2010; Thomas *et al*., 2012; among others).

On the contrary, very little is known about the provenance and tectonic evolution of the Chilenia terrane. Metamorphic rocks (Las Yaretas Gneisses) exposed west of the Guarguaraz area yield U-Pb ages in zircons between 1060 and 1080Ma (Ramos and Basei, 1997). Due to their age compatibility with Grenvillian rocks from Precordillera (Kay *et al*., 1996; Rapela *et al*., 2010), Ramos and Basei (1997) outlined two possible interpretations: i) Las Yaretas Gneisses belong to the Chilenia basement, and therefore,

Cuyania and Chilenia possibly derived from the same laurentian source or, ii) they represent imbricated slices of the basement of the Cuyania terrane emplaced into metasedimentary sequences located at Frontal Cordillera. Considering the last hypothesis as most likely, López de Azarevich *et al*. (2009) interpreted the Guarguaraz Complex as continental margin deposits of Vendian–early Cambrian age (~650–520Ma) developed along the western margin of the Cuyania terrane. Nevertheless, the two aforementioned hypotheses are still viable since no new compelling data are available. Therefore, the assignment of the Guarguaraz Complex to either the Cuyania or Chilenia terranes is currently a matter of debate. There is a general consensus that western Precordillera localities (Bonilla, Cortaderas, Peñasco) belong to the western margin of the Cuyania terrane (Ramos *et al*., 1984, 1986, among others). The Bonilla Complex is assigned to a continental margin setting and has a maximum sedimentation age of *ca*. 592Ma (Gregori *et al*., 2013), thus it can be considered temporarily equivalent to the Guarguaraz Complex, which yield a maximum sedimentation age of 555±8Ma (Willner *et al*., 2008). To the north, in the Cortaderas and Peñasco areas, the Cortadera Complex is similar to the Guarguaraz and Bonilla complexes regarding their lithology, structure, metamorphic grade, and their mafic-ultramafic association. The Cortadera Complex sedimentation age is not yet constrained, but Davis *et al*. (2000) dated in 576±17Ma (U-Pb on zircon) a metabasaltic dike that intrudes phyllites, hence its time span could be extended to the late Neoproterozoic and be a temporal equivalent of the Bonilla and Guarguaraz complexes.

The Neoproterozoic basaltic magmatism that intrude the metasedimentary successions show a N- and E-MORB chemical and mantle isotopic signatures, with εNd between +3.8 and +8.2 (Davis *et al*., 2000; López de Azarevich *et al*., 2009). Basei *et al*. (1997) and López de Azarevich *et al*. (2009) estimated Sm-Nd model ages (TDM) between 0.57 and 1.62Ga for mafic bodies from the Guarguaraz area, which are interpreted to represent a Grenvillian mantle source for this basaltic magmatism.

Serpentinites from different complexes exhibit similar geochemical fingerprints. The Peñasco serpentinites show subhorizontal HREE slopes, which evidence that they were originated out of the garnet stability field, a feature also observed in the Guarguaraz serpentinites (López and Gregori, 2004; López de Azarevich *et al*., 2009). Besides, Cr-spinel chemistry reveals that the Peñasco serpentinites show an intermediate signature between a mid-ocean ridge and an arc-related ophiolite. The presence of serpentinized ultramafic rocks along the suture zone between the Cuyania and Chilenia terranes (Guarguaraz, Cortadera and Bonilla complexes) spatially associated to a N- and E-MORB basaltic magmatism and continental margin metasedimentary successions evidence the development of an oceanic basin between the Cuyania and Chilenia terranes during the Neoproterozoic-early Paleozoic within an extensional regime associated to the Rodinia break-up.

Deformation associated with serpentinite obduction and tectonic emplacement related to the closure of the aforementioned oceanic basin generated faults, fractures and joints which constituted excellent pathways for hydrothermal fluids pervasive circulation. Serpentinization and listvenitization processes might have occurred during the opening and closure of the oceanic basin that separated the Chilenia and Cuyania terranes in Neoproterozoic-early Paleozoic times (Ramos *et al*., 1984, 1986; Davis *et al*., 1999, 2000; Willner *et al*., 2011).

CONCLUSIONS

In this contribution, we present the first geochemical whole-rock data set and the first chemical data set of Cr-spinels from the Cordón del Peñasco serpentinites.

Cr-spinels analyzed (picotite, pleonaste and spinel *sensu stricto*) show holly leaf shapes. They are chemically homogeneous and show mid-ocean ridge to arc affinities. They could have evolved from a mid-ocean ridge to an arc-related ophiolite related to the tectonic evolution of the Cuyania and Chilenia terranes.

Pseudomorphic textures formed by chrysotile/lizardite +magnetite±brucite±chlorite allow us to interpret that serpentinites derived from harzburgitic cumulates subjected to an ocean-floor hydrothermal alteration at temperatures ≤300ºC.

Multistage metasomatic processes involving carbonatization and listvenitization also affected the serpentinites. Ca, Sr, LREE (specially Eu) and MREE enrichments were generated by a hydrothermal/serpentinite interaction at T below 400ºC. The fluid was CO_2 and complexing ion (F^-, Cl^-, CO_3^{2-}, PO_4^{3-})-rich, with mildly basic conditions for REE complexation.

The presence of quartz in listvenite mineralogy suggests the occurrence of a second type of fluid with low pH, fO_2 and T~250ºC.

An extensional regime associated to the Rodinia break-up may have led to the development of an oceanic basin between the Chilenia and Cuyania terranes at Neoproterozoic–early Paleozoic times evidenced by the presence of the metasomatized serpentinite bodies studied here and the occurrence of N- to E-MORB magmatism coeval with continental margin sedimentation of that age.

ACKNOWLEDGEMENTS

This research has been developed within Florencia L. Boedo's PhD thesis and has been funded by research projects CONICET PIP 0072 and UBACyT 20020100100862 (Graciela Vujovich). The authors wish to thank Dr. Iris Díaz and Mr. Daniel Costa from the Servicio Geológico Minero Argentino (SEGEMAR) for logistic support during field activities. We are deeply grateful to Dr. Yuji Ichiyama, George Harlow and Tatsuki Tsujimori (Associated Editor) for their generous and helpful comments that really improved the early version of this manuscript. This is the R-164 contribution of the Instituto de Estudios Andinos Don Pablo Groeber.

REFERENCES

Abre, P., Cingolani, C.A., Cairncross, B., Chemale, F.Jr., 2012. Siliciclastic Ordovician to Silurian units of the Argentine Precordillera: Constraints on provenance and tectonic setting in the proto-Andean margin of Gondwana. Journal of South American Earth Sciences, 40, 1-22.

Akbulut, M., Piskin, O., Karayiğit, A., 2006. The genesis of the carbonatized and silicified ultramafics known as listvenites: a case study from the Mihaliccik region (Eskisehir), NW Turkey. International Geology Journal, 41, 557-580.

Allen, D.E., Seyfried, W.E.Jr., 2005. REE controls in ultramafic hosted MOR hydrothermal systems: an experimental study at elevated temperature and pressure. Geochimica et Cosmochimica Acta, 69(3), 675-683.

Arai, S., Okamura, H., Kadoshima, K., Tanaka, C., Suzuki, K., Ishimaru, S., 2011. Chemical characteristics of chromian spinel in plutonic rocks: implications for deep magma processes and discrimination of tectonic setting. Island Arc, 20, 157-137.

Astini, R.A., Benedetto, J., Vaccari, N., 1995. The Early Paleozoic evolution of the Argentine Precordillera as a Laurentian rifted, drifted and collided terrane: a geodynamic model. Geological Society of America Bulletin, 17, 253-273.

Barnes, S.J., Roeder, P.L., 2001. The range of spinel compositions in terrestrial mafic and ultramafic rocks. Journal of Petrology, 42(12), 2279-2302.

Basei, M., Ramos, V., Vujovich, G., Poma, S., 1997. El basamento metamórfico de la Cordillera Frontal de Mendoza: nuevos datos geocronológicos e isotópicos. 10° Congreso Latinoamericano de Geología y 6° Congreso Nacional de Geología Económica, 2, 412-417.

Bjerg, E.A., Gregori, D.A., Losada Calderón, A., Labadía, C.H., 1990. Las metamorfitas del faldeo oriental de la Cuchilla de Guarguaraz, Cordillera Frontal, Provincia de Mendoza. Revista Asociación Geológica Argentina, 45, 234-245.

Bodinier, J.L., Godard, M., 2003. Orogenic, ophiolitic and abyssal peridotites. In: Carlson, R. (ed.). Treatise on geochemistry 2: the mantle and core. Oxford, Elsevier-Pergamon, 103-170.

Boedo, F.L., Vujovich, G.I., Barredo, S.P., 2012. Caracterización de rocas ultramáficas, máficas y metasedimentarias del Cordón del Peñasco, Precordillera occidental, Mendoza. Revista Asociación Geológica Argentina, 69(2), 275-286.

Bromiley, G.D., Pawley, A.R., 2003. The stability of antigorite in the systems MgO-SiO_2-H_2O (MSH) and MgO-Al_2O_3-SiO_2-H_2O (MASH): The effects of Al3+ substitution on high-pressure stability. American Mineralogist, 88, 99-108.

Buggisch, W., Von Gosen, W., Henjes-Kunst, F., Krumm, S., 1994. The age of Early Paleozoic deformation and metamorphism in the Argentine Precordillera–Evidence from K-Ar data. Zentrablatt für Geologie und Palaontologie, 1, 275-286.

Coish, R.A., Gardner, P., 2004. Suprasubduction zone peridotite in northern USA Appalachians: evidence from mineral composition. Mineralogical Magazine, 68, 699-708.

Coleman, R.G., 1977. Ophiolites. Ancient oceanic lithosphere? Heidelberg, Springer-Verlag, 229pp.

Cortés, J.M., Kay, S.M., 1994. Una dorsal oceánica como origen de las lavas almohadilladas del Grupo Ciénaga del Medio (Silúrico-Devónico) de la Precordillera de Mendoza, Argentina. 7º Congreso Geológico Chileno, 2, 1005-1009.

Cucchi, R., 1971. Edades radimétricas y correlación de metamorfitas de la Precordillera, San Juan-Mendoza, República Argentina. Revista Asociación Geológica Argentina, 26, 503-515.

Cucchi, R., 1972. Geología y estructura de la Sierra de Cortaderas, San Juan-Mendoza, República Argentina. Revista Asociación Geológica Argentina, 27, 229-248.

Dalla Salda, L.H., Dalziel, I.W.D., Cingolani, C.A., Varela, R., 1992. Did the Taconic Appalachians continue into South America? Geology, 20, 1059-1062.

Davis, J., Roeske, S., McClelland, W., Snee, L., 1999. Closing an ocean between the Precordillera terrane and Chilenia: early Devonian ophiolite emplacement and deformation in the southwest Precordillera. In: Ramos, V., Keppie, J. (eds.). Laurentia-Gondwana connection before Pangea. Boulder, Geological Society, 336 (Special Paper), 115-138.

Davis, J., Roeske, S., McClelland, W., Kay, S.M., 2000. Mafic and ultramafic crustal fragments of the southwestern Precordillera terrane and their bearing on tectonic models of the early Paleozoic in western Argentina. Geology, 28, 171-174.

Deer, W.A., Howie, R.A., Zussman, J., 1962. Rock-forming minerals. Sheet Silicates. Wiley, 3, 270pp.

Deschamps, F., Godard, M., Guillot, S., Hattori, K., 2013. Geochemistry of subduction zone serpentinites: a review. Lithos, 178, 96-127.

Dick, H.J.B., Bullen, T., 1984. Chromian spinel as a petrogenetic indicator in abyssal and alpine-type peridotites and spatially associated lavas. Contributions to Mineralogy and Petrology, 86, 54-76.

Dickerson, P.W., 2012. The Circum-Laurentian Carbonate Bank, the Western Ouachita-Cuyania Basin and the Prodigal Llanoria Landmass. In: Derby, J., Fritz, R., Longacre, S., Morgan, W., Sternbach, C. (eds.). The great American carbonate bank: The geology and economic resources of the Cambrian-Ordovician

Sauk megasequence of Laurentia. American Association of Petroleum Geologists, 98 (Memoir), 959-984.

Droop, G.T.R., 1987. A general equation for estimating Fe3+ concentrations in ferromagnesian silicates and oxides from microprobe analyses, using stoichiometric data. Mineralogical Magazine, 51, 431-435.

Evans, B.W., 1977. Metamorphism of alpine peridotite and serpentinite. Annual Review of Earth and Planetary Science, 5, 397-447.

Evans, B.W., 2004. The serpentinite multisystem revisited: chrysotile is metastable. International Geology Review, 46, 479-506.

Fauqué, L.E., Villar, L.M., 2003. Reinterpretación estratigráfica y petrología de la Formación Chuscho, Precordillera de La Rioja. Revista Asociación Geológica Argentina, 58(2), 218-232.

Gargiulo, M.F., Bjerg, E.A., Mogessie, A., 2011. Caracterización y evolución metamórfica de las rocas ultramáficas de la Faja del río de las Tunas, Cordillera Frontal de Mendoza. Revista Asociación Geológica Argentina, 68(4), 571-593.

Gargiulo, M.F., Bjerg, E.A., Mogessie, A., 2013. Spinel group minerals in metamorphosed ultramafic rocks from Rio de Las Tunas belt, Central Andes, Argentina. Geologica Acta, 11(2), 133-148.

Gerbi, C., Roeske, S.M., Davis, J.S., 2002. Geology and structural history of the southwestern Precordillera margin, northern Mendoza Province, Argentina. Journal of South American Earth Sciences, 14, 821-835.

Gregori, D.A., Bjerg, E.A., 1997. New evidence on the nature of the Frontal Cordillera ophiolitic belt-Argentina. Journal of South American Earth Sciences, 10(2), 147-155.

Gregori, D.A., Martinez, J.C., Benedini, L., 2013. The Gondwana-South America Iapetus margin evolution as recorded by Lower Paleozoic units of western Precordillera, Argentina: the Bonilla Complex, Uspallata. Serie Correlación Geológica, 29(1), 21-80.

Haggerty, S.E., 1991. Oxide mineralogy of the upper mantle. Spinel mineral group. In: Lindsley, D.H. (ed.). Reviews in Mineralogy, Oxide minerals: Petrologic and magnetic significance. Mineralogical Society of America, 25, 355-416.

Haller, M.J., Ramos, V.A., 1984. Las ofiolitas famitinianas (Eopaleozoico) de las provincias de San Juan y Mendoza. 9º Congreso Geológico Argentino, 3, 66-83.

Halls, C., Zhao, R., 1995. Listvenite and related rocks: perspectives on terminology and mineralogy with reference to an occurrence at Cregganbaun, Co. Mayo, Republic of Ireland. Mineralium Deposita, 30, 303-313.

Harrington, H.J., 1971. Hoja Geológica 22c Ramblón. Boletín 114. Buenos Aires, Dirección Nacional de Geología y Minería, 81pp.

Irvine, T.N., 1967. Chromian spinels as a petrogenentic indicator. Part 2 Petrologic applications. Canadian Journal of Earth Sciences, 4, 71-103.

Kamenetsky, V.S., Crawford, A.J., Meffre, S., 2001. Factors controlling chemistry of magmatic spinel: an empirical study of associated olivine, Cr-spinel and melt inclusions from primitive rocks. Journal of Petrology, 42, 655-671.

Kay, S.M., Orrell, S., Abbruzzi, J.M., 1996. Zircon and whole-rock Nd-Pb isotopic evidence for a Grenville age and Laurentian origin for the basement of the Precordilleran terrane in Argentina. Journal of Geology, 104, 637-648.

Kay, S.M., Ramos, V.A., Kay, R., 1984. Elementos mayoritarios y trazas de las vulcanitas ordovícicas de la Precordillera occidental; basaltos de rift oceánico temprano(?) próximo al margen continental. 9º Congreso Geológico Argentino, 2, 48-65.

Kodolànyi, J., Pettke, T., Spandler, C., Kamber, B.S., Gméling, K., 2012. Geochemistry of ocean floor and fore-arc serpentinites: constraints on the ultramafic input to subduction zones. Journal of Petrology, 53(2), 235-270.

Loeske, W.P., 1993. La Precordillera del oeste argentino: una cuenca de back arc en el Paleozoico. 12º Congreso Geológico Argentino, 1, 5-13.

López, V.L., Gregori, D.A., 2004. Provenance and evolution of the Guarguaraz complex, Cordillera Frontal, Argentina. Gondwana Research, 7, 1197-1208.

López de Azarevich, V., Escayola, M., Azarevich, M.B., Pimentel, M.M., Tassinari C., 2009. The Guarguaraz Complex and the Neoproterozoic-Cambrian evolution of southwestern Gondwana: Geochemical signatures and geochronological constraints. Journal of South American Earth Sciences, 28, 333-344.

Massonne, H.-J., Calderón, M., 2008. P-T evolution of metapelites from the Guarguaraz Complex, Argentina: evidence for Devonian crustal thickening close to the western Gondwana margin. Revista Geológica de Chile, 35(2), 215-231.

Mellini, M., Trommsdorff, V., Compagnoni, R., 1987. Antigorite polysomatism: behaviour during progressive metamorphism. Contributions to Mineralogy and Petrology, 97, 147-155.

Menzies, M., Long, A., Ingram, G., Tatnell, M., Janecky, D.R., 1993. MORB peridotite–seawater interaction: experimental constraints on the behaviour of trace elements, 87Sr/86Sr and 143Nd/144Nd ratios. In: Prichard, H.M., Alabaster, T., Harris, N.B.W., Neary, C.R. (eds.). Magmatic Processes and Plate Tectonics. London, Geological Society Special Publication, 76, 309-322.

Mukherjee, R., Mondal, S.K., Rosing, M.T., Frei, R., 2010. Compositional variations in the Mesoarchean chromites of the Nuggihalli schist belt, Western Dharwar Craton (India): potential parental melts and implications for tectonic setting. Contributions to Mineralogy and Petrology, 160, 865-885.

Naipauer, M., Vujovich, G.I., Cingolani, C.A., McClelland, W.C., 2010. Detrital zircon analysis from the Neoproterozoic–Cambrian sedimentary cover (Cuyania Terrane), Sierra de Pie de Palo, Argentina: Evidence of a rift and passive margin system? Journal of South American Earth Sciences, 29(2), 306-326.

Paulick, H., Bach, W., Godard, M., De Hoog, J.C.M., Suhr, G., Harvey, J., 2006. Geochemistry of abbysal peridotites (Mid-Atlantic Ridge, 15º20'N, ODP Leg 209): implications

for fluid/rock interaction in slow spreading environments. Chemical Geology, 234, 179-210.

Pearce, J.A., Barker, P.F., Edwards, S.J., Parkinson, I.J., Leat, P.T., 2000. Geochemistry and tectonic significance of peridotites from the South Sandwich arc-basin system, South Atlantic. Contributions to Mineralogy and Petrology, 139, 36-53.

Ramos, V.A., 2010. The Grenville-age basement of the Andes. Journal of South American Earth Sciences, 29, 77-91.

Ramos, V.A., Basei, M., 1997. The basement of Chilenia: an exotic continental terrane to Gondwana during the Early Paleozoic. In: Bradshaw, J.D., Weaver, S.D. (eds.). Terrane dynamics 97. International Conference on Terrane Geology, 140-143.

Ramos, V.A, Escayola, M., Mutti, D., Vujovich, G.I., 2000. Proterozoic-Early Paleozoic ophiolites of the Andean basement of southern South America. Ophiolitic and Oceanic Crust: new insights from field studies and the Ocean Drilling Program. Boulder, Geological Society, 349 (Special Paper), 331-349.

Ramos, V.A., Jordan, T., Allmendinger, R., Kay, S., Cortes, J.M., Palma, M., 1984. Chilenia: un terreno alóctono en la evolución paleozoica de los Andes Centrales. 9º Congreso Geológico Argentino, 2, 84-106.

Ramos, V.A., Jordan, T.E., Allmendinger, R.W., Mpodozis, C., Kay, S.M., Cortes, J.M., Palma, M., 1986. Paleozoic terranes of the Central Argentine-Chilean Andes. Tectonics, 5, 855-880.

Rapela, C.W., Pankhurst, R.J., Casquet, C., Baldo, E., Galindo, C., Fanning, C.M., Dahlquist, J., 2010. The Western Sierras Pampeanas: Protracted Grenville-age history (1330–1030Ma) of intra-oceanic arcs, subduction–accretion at continental edge and AMCG intraplate magmatism. Journal of South American Earth Sciences, 29, 105-127.

Robinson, P.T., Malpas, J., Zhou, M., Ash, C., Yang, J., Bai, W., 2005. Geochemistry and origin of listwanites in the Sartohay and Luobusa ophiolites, China. International Geology Review, 47, 177-202.

Rose, G., 1837. Mineralogisch-geognostiche Reise nach dem Ural, dem Altai and dem Kaspischen Meere. In: Eichhoff, C.W. (ed.). Reise nach dem sudlichen Ural und dem Altai. Berlin, Verlag der Sanderschen Buchhandlung, 1, 648pp.

Singh, A.K., Singh, R.B., 2013. Genetic implications of Zn- and Mn-rich Cr-spinels in serpentinites of the Tidding Suture Zone, eastern Himalaya, NE India. Geological Journal, 48, 22-38.

Spear, F.S., 1995. Metamorphic phase equilibria and Pressure-Temperature-Time paths. Washington DC, Mineralogical Society of America Monograph, 1, 799pp.

Sun, S., McDonough, W., 1989. Chemical and isotopic systematics of oceanic basalts: implications for mantle composition and processes. Magmatism in the Ocean Basins. London, Geological Society, 42 (Special Publication), 313-345.

Taylor, S., McLennan, S., 1985. The Continental Crust: its composition and evolution. An examination of the geochemical record preserved in sedimentary rocks. Oxford, Blackwell, 312pp.

Thomas, W.A., Astini, R.A., 2003. Ordovician accretion of the Argentine Precordillera terrane to Gondwana: a review. Journal of South American Earth Sciences, 16, 67-79.

Thomas, W.A., Tucker, R.D., Astini, R.A., Denison, R.E., 2012. Ages of pre-rift basement and synrift rocks along the conjugate rift and transform margins of the Argentine Precordillera and Laurentia. Geosphere, 8(6), 1-18.

Tsikouras, B., Karipi, S., Grammatikopoulos, T.A., Hatzipanagiotou, K., 2006. Listwaenite evolution in the ophiolite melange of Iti Mountain (continental Central Greece). European Journal of Mineralogy, 18, 243-255.

Uçurum, A., 2000. Listwaenites in Turkey: perspectives on formation and precious metal concentration with reference to occurrences in east-central Anatolia. Ofioliti, 25(1), 15-29.

Villar, L.M., 1969. El complejo ultrabásico de Novillo Muerto, Cordillera Frontal, Provincia de Mendoza, República Argentina. Revista Asociación Geológica Argentina, 24, 223-238.

Villar, L.M., 1970. Petrogénesis del complejo ultrabásico de Novillo Muerto, Cordillera Frontal, Mendoza, Argentina. Revista Asociación Geológica Argentina, 25, 87-99.

Von Gosen, W., 1997. Early Paleozoic and Andrean structural evolution in the Rio Jáchal section of the Argentine Precordillera. Journal of South American Earth Sciences, 10, 361-388.

Whitney, D.L., Evans, B.W., 2010. Abbreviations for names of rock-forming minerals. American Mineralogist, 95, 185-187.

Willner, A.P., Gerdes, A., Massonne, H.-J., 2008. History of crustal growth and recycling at the Pacific convergent margin of South America at latitudes 29°-36°S revealed by a U-Pb and Lu-Hf isotope study of detrital zircon from late Paleozoic accretionary systems. Chemical Geology, 253, 114-129.

Willner, A.P. Gerdes, A., Massonne, H.-J., Schmidt, A., Sudo, M., Thomson, S.N., Vujovich, G., 2011. The geodynamics of collision of a microplate (Chilenia) in Devonian times deduced by the pressure-temperature-time evolution within part of a collisional belt (Guarguaraz Complex, W-Argentina). Contributions to Mineralogy and Petrology, 162, 303-327.

Winkler, H., 1978. Petrogénesis de rocas metamórficas. Madrid, Blume Ediciones, 346pp.

Wood, S.A., 1990. The aqueous geochemistry of the rare-earth elements and yttrium. I. Review of available low temperature data for inorganic complexes and the inorganic REE speciation of natural waters. Chemical Geology, 82, 159-186.

Wunder, B., Wirth, R., Gottschalk, M., 2001. Antigorite: Pressure and temperature dependence of polysomatism and water content. European Journal of Mineralogy, 13, 485-495.

Manuscript received December 2014;
revision accepted June 2015;
publishede Online July 2015.